Stability and time-domain analysis of the dispersive tristability in microresonators under modal coupling

Yannick Dumeige* and Patrice Féron
Université Européenne de Bretagne, Laboratoire Foton and
CNRS, UMR 6082 Foton, Enssat, BP 80518, F-22305 Lannion Cedex, France
(Received 29 April 2011; published 28 October 2011)

Coupled nonlinear resonators have potential applications for the integration of multistable photonic devices. The dynamic properties of two coupled-mode nonlinear microcavities made of Kerr material are studied by linear stability analysis. Using a suitable combination of the modal coupling rate and the frequency detuning, it is possible to obtain configurations where a hysteresis loop is included inside other bistable cycles. We show that a single resonator with two modes both linearly and nonlinearly coupled via the cross-Kerr effect can have a multistable behavior. This could be implemented in semiconductor nonlinear whispering-gallery-mode microresonators under modal coupling for all optical signal processing or ternary optical logic applications.

DOI: 10.1103/PhysRevA.84.043847 PACS number(s): 42.55.Sa, 42.65.Pc, 42.65.Sf

I. INTRODUCTION

Nonlinear mirocavities are of great interest for applications in nonlinear photonics. In particular, multistable integrated optoelectronic systems could have applications in all-optical logic or memories [1,2]. Due to recent technological progress made in the fabrication of high-Q microresonators, it is now possible to consider photonic devices or functions involving several coupled microcavities with low losses and fast optical nonlinearities. In the linear regime, the coupling of resonators is used to improve and tailor the filtering properties compared with single-microresonator approaches. For example, high-order band-pass filters with flat transmission and group delay dispersion have been proposed [3,4]. The coupling of resonators also increases the possibility offered by nonlinear microcavities. In second-order nonlinear processes, it allows the quasi-phase-matching condition to be reached [5–7]. Third-order nonlinear frequency conversion can be enhanced in a coupled-resonator optical waveguide [8]. The coupling between resonators can be chosen in order to optimize the nonlinear or dynamic properties of all-optical signal processing functions [9,10]. For example, cascaded sets of nonlinear microresonators can control the pulse distortion in miniaturized optical gates for pulse reshaping [11]. The stationary response of coupled nonlinear resonators shows potential multistable behavior [12], but the linear stability analysis of such configurations has not been achieved yet. It has also been theoretically demonstrated that coupled third-order nonlinear microcavities have self-pulsing or chaotic behavior [13,14]. Recently, an interpretation of this phenomenon has been proposed: the self-pulsing originates from the counteraction of mode beating and bistable switching [15]. From another point of view, interesting switching processes have been proposed using nonreciprocal effects in arrays of nonlinear microresonators [16]. Symmetry breaking can occur in two coupled microresonators made of Kerr material pumped by two degenerate beams. This effect can be exploited for all-positive pulse switching [17]. In some particular configurations a single microresonator under modal coupling can behave as a coupled-cavity system. This has been demonstrated in a semiconductor laser microdisk where the interplay between the two counterpropagating modes leads to very interesting switching schemes [1]. Modal coupling can also be observed in passive microresonators: enhanced Rayleigh backscattering can couple the two counterpropagating modes of a whispering-gallery-mode (WGM) resonator [18–23]. The nonlinear properties of such a two-mode system have already been studied in the framework of nonlinear effects based on two-photon absorption and plasma carrier dispersion [24]. In this last study, the self-pulsation regime has been observed and well understood using the coupled-mode theory (CMT) [25]. In this paper we report on the study of the instantaneous third-order optical nonlinear properties (Kerr effect) of WGM microcavities under modal coupling. We have deduced from linear stability analysis and time-domain calculations that these systems can have a true multistable response.

This paper is organized as it follows. In Sec. II, we first give the formulation of the CMT applied to a coupled nonlinear two-cavity system modeling the two nonlinear WGMs (clockwise and counterclockwise) of the microresonator. Section III focuses on the stationary response of the studied system. We recall the basic linear properties of a two-mode cavity. The CMT is applied to calculate the nonlinear stationary response of the coupled-mode cavity. From the stationary response expression, we carry out the linear stability analysis of the system. In Sec. IV, using the linear stability analysis and time-domain calculations, we show that a device comprising two nonlinear modes both linearly and nonlinearly coupled can have a true multistable behavior.

II. MODAL-COUPLING MODEL

As represented in Fig. 1, we consider a single WGM cavity with two degenerated counterpropagating modes. The distributed linear coupling between the two modes comes from the enhanced Rayleigh backscattering, as already observed in several WGM resonator configurations [18–23]. It could also come from an artificial intracavity diffractive process, such as distributed Bragg reflection. In this configuration, since the two modes share the same cavity, they are also coupled via

*yannick.dumeige@univ-rennes1.fr

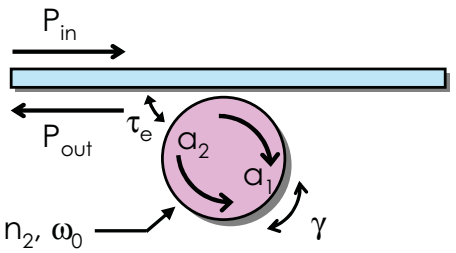

FIG. 1. (Color online) WGM nonlinear resonator with nonlinear index n_2 and coupling rate. The two counterpropagating modes a_1 and a_2 have the same resonant angular frequency ω_0; $1/(2\gamma)$ is their mutual coupling rate. They are also coupled with a characteristic time τ_e to a single access lines. P_{in} and P_{out} are, respectively, the input and output powers. The two modes share the same cavity authorizing nonlinear coupling via the cross-Kerr effect.

the cross-Kerr effect. The linear and nonlinear properties of the cavity are characterized by its resonant angular frequency ω_0 and its intrinsic amplitude lifetime τ_0. The coupling rate between the two modes of amplitude a_1 and a_2 is $1/(2\gamma)$; the coupling lifetime between the cavity mode and the bus waveguide fields is τ_e. Note that $|a_1|^2$ and $|a_2|^2$ correspond to the mode energies. The output field power P_{out} is related to the intracavity mode energy by

$$P_{\text{out}} = \frac{2}{\tau_e}|a_2|^2. \tag{1}$$

The equations of motion of the mode amplitudes read [19,23,25]

$$\begin{aligned} \frac{da_1}{dt} &= \left[j(\omega_0+\Delta\omega_1)-\frac{1}{\tau}\right]a_1+\frac{j}{2\gamma}a_2+\sqrt{\frac{2}{\tau_e}}s_{\text{in}}, \\ \frac{da_2}{dt} &= \left[j(\omega_0+\Delta\omega_2)-\frac{1}{\tau}\right]a_2+\frac{j}{2\gamma}a_1, \end{aligned} \tag{2}$$

where $\Delta\omega_i$ with $i \in \{1,2\}$ are the nonlinear frequency shifts due to the Kerr effect. Equations (2) would also be used to model a two-coupled-cavity system. The difference between the two cases would come from the expressions of the nonlinear frequency shift. For a two-cavity system would write $\Delta\omega_i = q|a_i|^2$, whereas the nonlinear shifts of the cavity resonance are given by $\Delta\omega_1 = q|a_1|^2 + 2q|a_2|^2$ and $\Delta\omega_2 = 2q|a_1|^2 + q|a_2|^2$ for the distributed coupling configuration analyzed in this paper, taking into account the cross-Kerr effect [12,26]. The parameter q depends on n_{eff}, the effective refractive index of the mode, and n_2, the nonlinear refraction index of the material, constituting the cavity and its mode volume $\mathcal{V}$ by [27]

$$q = \frac{n_2\omega_0 c}{n_{\text{eff}}^2\mathcal{V}}. \tag{3}$$

Note that in this work, we limit our theoretical analysis to instantaneous third-order nonlinear effects. In Eqs. (2), τ is the overall lifetime of the field inside the cavity, and it can be written

$$\frac{1}{\tau} = \frac{1}{\tau_0}+\frac{1}{\tau_e}. \tag{4}$$

Finally, s_{in} is the input field related to the input power P_{in} by $P_{\text{in}} = |s_{\text{in}}|^2$.

In the aim of a thorough device design, the CMT must be combined with full numerical calculations, such as the finite-difference time-domain method (FDTD). The FDTD can be used to determine all the effective parameters, for example, τ, γ, and $\mathcal{V}$. The FDTD method including third-order nonlinear susceptibility is also useful for the verification of the CMT nonlinear calculations. In most cases a good agreement can be found between the results of the CMT and the FDTD results [28–30], even in the case of coupled cavities [13]. This validates the use of the CMT to get the physical insight into complex coupled-resonator photonic devices without long time consumption. The coupling coefficients may also be derived from full Maxwell equations by perturbative calculations [31,32]. In this paper we do not carry out numerical calculations and limit our calculations to stationary and time-domain CMT approaches.

III. STATIONARY RESULTS

A. Linear properties

We first focus on the linear stationary regime ($q = 0$). In this case, the excitation of the system can be chosen as $s_{\text{in}}(t) = S_{\text{in}}\exp(j\omega t)$, where ω is the excitation angular frequency related to the cavity resonance by $\Omega = \omega - \omega_0$, where Ω is defined as the angular frequency detuning. The properties of the structure are given by the power transfer function $T = P_{\text{out}}/P_{\text{in}}$ of the device, which reads [23]

$$T(\Omega) = \frac{1/\left(\gamma^2\tau_e^2\right)}{\left[\left(\Omega+\frac{1}{2\gamma}\right)^2+\frac{1}{\tau^2}\right]\left[\left(\Omega-\frac{1}{2\gamma}\right)^2+\frac{1}{\tau^2}\right]}. \tag{5}$$

For sufficiently large coupling rates, $\frac{1}{\gamma} > \frac{2}{\tau}$, this linear transmission spectrum displays two split resonance frequencies obtained for

$$\Omega = \pm\frac{1}{2\gamma}\sqrt{1-\left(\frac{2\gamma}{\tau}\right)^2}. \tag{6}$$

This is illustrated in Fig. 2, where we give the linear transfer function of the system for a lossless material ($\tau_0 \to +\infty$). Figure 2(a) is obtained for $\tau = 2\gamma$ (critical coupling [19]), and the transmission spectrum shows a flat profile at resonance, whereas Fig. 2(b) illustrates the case $\tau > 2\gamma$, where two well-separated resonance frequencies appear. It has already been proposed to use this interesting feature to reduce the required power to observe optical multistability [33] in passive systems [12].

B. Nonlinear response

Denoting $a_1(t) = A_1(t)e^{j\omega t}$ and $a_2(t) = A_2(t)e^{j\omega t}$, the nonlinear stationary transfer function of the structure is calculated from the static solutions $\overline{A}_1 = \overline{x}_1 + j\overline{y}_1$ and $\overline{A}_2 = \overline{x}_2 + j\overline{y}_2$ using $\overline{A}_2$ as a parameter. For convenience and without loss of generality we chose $\overline{A}_2$ real and positive and then $\overline{y}_2 = 0$. The imaginary part of $\overline{A}_1$ is then given by

$$\overline{y}_1 = -\frac{2\gamma}{\tau}\overline{x}_2, \tag{7}$$

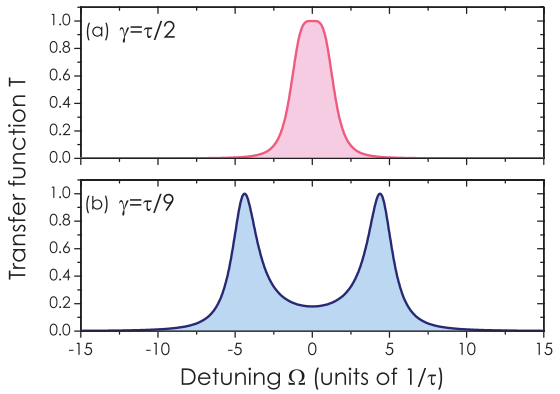

FIG. 2. (Color online) Linear power transfer function $T = P_{\text{out}}/P_{\text{in}}$ in the case of lossless cavities ($\tau_0 \to +\infty$) for two different coupling rates: (a) $\gamma = \tau/2$ and (b) $\gamma = \tau/9$.

and the real part $\overline{x}_1$ is obtained by solving

$$\overline{x}_1^2 + \frac{1}{4q\gamma\overline{x}_2}\overline{x}_1 + \overline{x}_2^2\left[\left(\frac{2\gamma}{\tau}\right)^2 + \frac{1}{2}\right] - \frac{\Omega}{2q} = 0. \tag{8}$$

In the general case, this equation has two solutions, which give two branches to the nonlinear stationary response of the single-cavity system. The input and output powers are thus given by

$$P_{\text{in}} = \frac{\tau_e}{2}\left|\frac{\overline{A}_2}{2\gamma} + \overline{A}_1\left(q|\overline{A}_1|^2 + 2q|\overline{A}_2|^2 - \Omega + \frac{j}{\tau}\right)\right|^2, \qquad P_{\text{out}} = \frac{2}{\tau_e}|\overline{A}_2|^2. \tag{9}$$

To analyze the stability of the static solutions obtained from Eq. (9) we study the evolution of first-order perturbations $X = (\delta\overline{x}_1, \delta\overline{y}_1, \delta\overline{x}_2, \delta\overline{y}_2)^T$ of the static solution $(\overline{A}_1, \overline{A}_2)$. The analysis of the eigenvalues of the Jacobian $\mathbf{J}$, defined by

$$\frac{dX}{dt} = \mathbf{J} \cdot X, \tag{10}$$

gives the stability of the static solutions. If all the eigenvalues have a negative real part, the static solution is stable. If one of the eigenvalues has a positive real part, one has to examine two cases: (i) the eigenvalue is real and (ii) the eigenvalue is complex. In case (i) the solution is unstable, and the system can evolve toward another state. Case (ii) is more complicated; the solution presents some oscillations and can exhibit self-pulsing, quasiperiodic, or chaotic behavior [13,34].

IV. MULTISTABLE TWO-MODE MICRORESONATORS

When the two coupled modes share the same cavity, one has to take into account both linear and nonlinear coupling via the Rayleigh backscattering and the cross-Kerr effect. This strongly affects the nonlinear shifts. Consequently, the nonlinear characteristics are strongly modified in comparison with bistable single nonlinear cavities. Figure 3 shows nonlinear characteristics (for several detunings Ω) of a two-mode cavity described in Fig. 1 in the case of the critical coupling ($\gamma = \tau/2$). For a moderate detuning ($\Omega = 3/\tau$), the cavity has mainly a bistable behavior, whereas for a large detuning

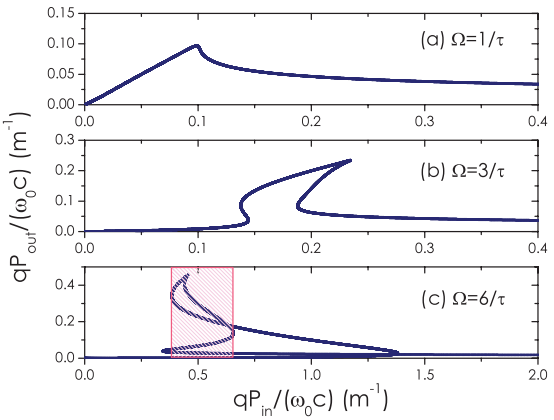

FIG. 3. (Color online) Normalized output power as a function of the normalized input power in the case of critical coupling ($\gamma = \tau/2$) for three different detuning: (a) $\Omega = 1/\tau$, (b) $\Omega = 3/\tau$, and (c) $\Omega = 6/\tau$. The potentially multistable area is hatched.

($\Omega = 6/\tau$) a multistable regime [hatched area in Fig. 3(c)] is potentially observable. Inspection of Fig. 3(c) reveals that all the stable states of the multistable area are not easily reachable using realistic input signals starting from zero. Increasing the modal coupling allows the multistable regime to be obtained. Figure 4 represents some nonlinear characteristics of a two-mode nonlinear cavity with a stronger modal coupling ($\gamma = \tau/9$) for three different detuning values. For weak detuning ($\Omega = 3/\tau$) the system is only bistable. Increasing the detuning, as in Fig. 4(b), a second hysteresis loop appears for low input powers. Finally, for a sufficiently large detuning (larger than $8/\tau$) the two hysteresis loops overlap, and the system becomes multistable, as shown by the hatched area in Fig. 4(c).

In Fig. 5 we detailed the output-power characteristic already represented in Fig. 4(c). In particular, we also give the stability analysis results. Note that the modal coupling used in this theoretical study is equivalent to that observed in AlGaAs microdisks by Michael *et al.* [22]. The two branches of the characteristic coming from $P_{\text{in}} \to 0$ and $P_{\text{in}} \to +\infty$ given

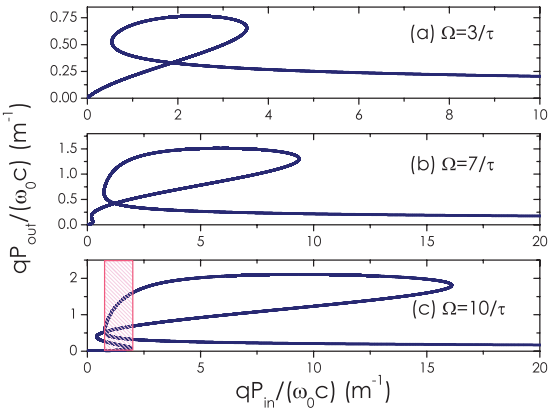

FIG. 4. (Color online) Normalized output power as a function of the normalized input power in the case of a strong modal coupling and frequency splitting ($\gamma = \tau/9$) for three different detunings: (a) $\Omega = 3/\tau$, (b) $\Omega = 7/\tau$, and (c) $\Omega = 10/\tau$. The potentially multistable area is hatched.

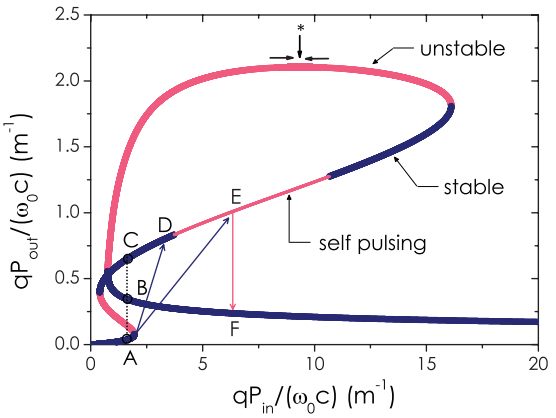

FIG. 5. (Color online) Normalized output power as a function of the normalized input power in the case of a single cavity supporting two coupled modes with $\gamma = \tau/9$ and $\Omega = 10/\tau$. For each solution we also give the linear stability analysis result.

by the two solutions of Eq. (8) join together at the point highlighted by the arrows and the asterisk. In the multistable area, tristability (i.e., three potentially stable states for the same input intensity) can be reached, as illustrated by the three characteristic points A, B, and C. We check it by direct integration of Eqs. (2) using the three input signals given in Fig. 6(a). Point A is reached by continuously increasing the input power from 0 to 1.7, as represented by time series (i) in Fig. 6(a). It is possible to reach point B by increasing the input power to enter the self-pulsing area (point E). At this point the system spontaneously jumps to the lowest branch (point F), and point B is then reached by decreasing the input power to 1.7 [time series (iii)]. Finally, still increasing the input power from A, the system jumps to D; then decreasing the input power, the system goes to state C [time series (ii)]. The final normalized input power of the three series is 1.7, whereas the output power reached in the three cases is different. The system acts as a true tristable system and could have applications in ternary optical logic, for instance [35,36].

Finally, in Fig. 7, we give the input and output time series for the same structure and input powers as those used in the previous tristable configuration. The only change is the input sequence: in this example we first reach point D before

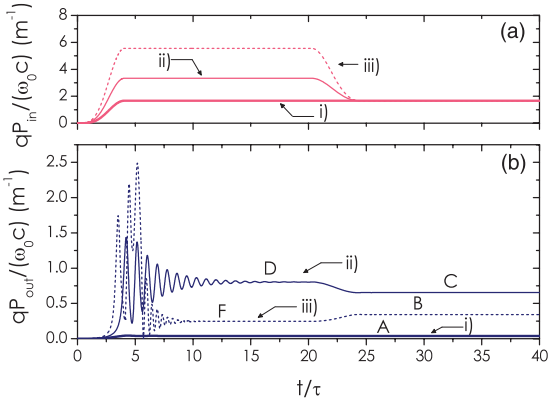

FIG. 6. (Color online) (a) Normalized input signal time series allowed to reach the three points A [series (i)], B [series (ii)], and C [series (iii)]. (b) Corresponding output signals.

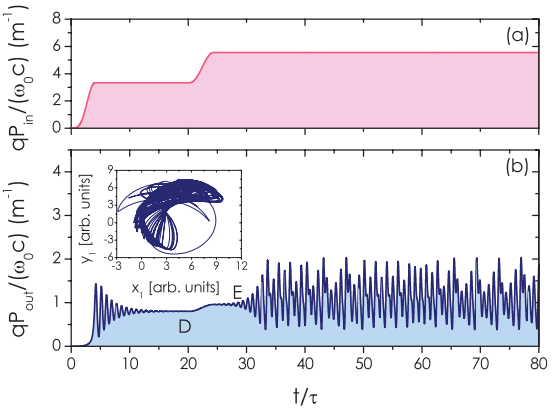

FIG. 7. (Color online) (a) Normalized input signal time series allowed to reach a quasiperiodic regime. (b) Corresponding output signals. In the inset we have plotted the phase portrait $y_1 = f(x_1)$.

point E. The inset shows the phase portrait $y_1 = f(x_1)$ of the associated output signal. This simulation shows that a quasiperiodic behavior [13] can be observed by reaching point E from point D. We thus emphasize that the system is sensitive to the time profile of the input signal. In the aim of practical applications, the input excitation profile must be thoroughly designed in order to avoid undesirable responses.

All the calculations have been made assuming a quality factor $Q = \omega_0\tau/2 = 3000$ ($\tau \approx 4.9$ ps at $\lambda_0 = 1.55$ μm) compatible with fast optical signal processing applications. Assuming, for example, AlGaAs microdisks (the Al composition of the alloy must be chosen to avoid the two-photon absorption to favor the Kerr effect) with $n_2 = 2 \times 10^{-13}$ cm^2/W [37], $n_{\text{eff}} = 2$, $\mathcal{V} = 6(\frac{\lambda_0}{n_0})^3$, where $n_0 = 3$ [38], we obtain a bias power (normalized input power around $P_{\text{in}} = 1.7$ for A, B, and C) around 280 mW. This input power would be considerably reduced using fast resonant nonlinearities, such as those based on the two-photon absorption and the free carrier dispersion in III-V semiconductors [39]. In this case the overall dynamic of the system would be strongly modified by the carrier dynamic [34]. Another way to reduce the input power consists in using hybrid systems [40] involving semiconductors and high intrinsic nonlinear susceptibility and low two-photon absorption polymer materials, such as *p*-toluene sulphonate (PTS) with $n_2 = 2.2 \times 10^{-12}$ cm^2/W at $\lambda_0 = 1.6$ μm [41]. By choosing higher Q factors (around 10^5, as reported in Ref. [22]) the required input power would be strongly reduced at the expense of the pulse duration.

V. CONCLUSION

The coupled-mode theory is a simple tool allowing the dynamical response of coupled nonlinear cavities to be simulated. The model requires only effective parameters that could be inferred using full numerical linear methods. We have applied this model to study the nonlinear response of a single Kerr microcavity with modal coupling. Stability analysis and direct time-domain integration show that such a microresonator can operate as a true tristable nonlinear photonic device. The study must be extended to fast, but finite, response time nonlinear processes to propose coupled-resonator architectures requiring weaker optical input powers [34].

ACKNOWLEDGMENTS

We acknowledge support by the EU through Project No COPERNICUS (FP-ICP-249012), and the French Agence Nationale de la Recherche through Project No CALIN (ANR 2010 BLAN-1002-02) and Project No ORA (ANR 2010 BLAN-0312-01). We would like also to acknowledge anonymous referees for useful comments.

[1] L. Liu, R. Kumar, K. Huybrechts, T. Spuesens, G. Roelkens, E.-J. Geluk, T. de Vries, P. Regreny, D. van Thourhout, R. Baets, and G. Morthier, Nat. Photonics **4**, 182 (2010).
[2] T. Paraïso, M. Wouters, Y. Léger, F. Morier-Genoud, and B. Deveaud-Plédran, Nat. Mater. **9**, 655 (2010).
[3] B. E. Little, S. T. Chu, J. V. Hryniewicz, and P. P. Absil, Opt. Lett. **25**, 344 (2000).
[4] V. Van, J. Lightwave Technol. **24**, 2912 (2006).
[5] Y. Xu, R. K. Lee, and A. Yariv, J. Opt. Soc. Am. B **17**, 387 (2000).
[6] Y. Dumeige, Opt. Lett. **32**, 3438 (2007).
[7] Y. Dumeige, Phys. Rev. A **83**, 045802 (2011).
[8] A. Melloni, F. Morichetti, and M. Martinelli, J. Opt. Soc. Am. B **25**, C87 (2008).
[9] J. E. Heebner, R. W. Boyd, and Q.-H. Park, Phys. Rev. E **65**, 036619 (2002).
[10] A. Melloni, F. Morichetti, and M. Martinelli, Opt. Quantum Electron. **35**, 365 (2003).
[11] Y. Dumeige, L. Ghisa, and P. Féron, Opt. Lett. **31**, 2187 (2006).
[12] Y. Dumeige and P. Féron, Phys. Rev. E **72**, 066609 (2005).
[13] B. Maes, M. Fiers, and P. Bienstman, Phys. Rev. A **80**, 033805 (2009).
[14] J. Petráček, A. Sterkhova, and J. Luksch, Microwave Opt. Technol. Lett. **53**, 2238 (2011).
[15] V. Grigoriev and F. Biancalana, Phys. Rev. A **83**, 043816 (2011).
[16] K. Huybrechts, G. Morthier, and B. Maes, J. Opt. Soc. Am. B **27**, 708 (2010).
[17] B. Maes, M. Soljačić, J. D. Joannopoulos, P. Bienstman, R. Baets, S.-P. Gorza, and M. Haelterman, Opt. Express **14**, 10678 (2006).
[18] D. S. Weiss, V. Sandoghdar, J. Hare, V. Lefèvre-Seguin, J.-M. Raimond, and S. Haroche, Opt. Lett. **20**, 1835 (1995).
[19] T. J. Kippenberg, S. M. Spillane, and K. J. Vahala, Opt. Lett. **27**, 1669 (2002).
[20] M. Borselli, K. Srinivasan, P. E. Barclay, and O. Painter, Appl. Phys. Lett. **85**, 3693 (2004).
[21] A. Mazzei, S. Götzinger, L. de S. Menezes, G. Zumofen, O. Benson, and V. Sandoghdar, Phys. Rev. Lett. **99**, 173603 (2007).
[22] C. P. Michael, K. Srinivasan, T. J. Johnson, O. Painter, K. H. Lee, K. Hennessy, H. Kim, and E. Hu, Appl. Phys. Lett. **90**, 051108 (2007).
[23] S. Trebaol, Y. Dumeige, and P. Féron, Phys. Rev. A **81**, 043828 (2010).
[24] T. J. Johnson, M. Borselli, and O. Painter, Opt. Express **14**, 817 (2006).
[25] H. A. Haus, *Waves and Fields in Optoelectronics* (Prentice-Hall, Englewood Cliffs, NJ, 1984).
[26] M. Yanik, H. Altug, J. Vuckovic, and S. Fan, J. Lightwave Technol. **22**, 2316 (2004).
[27] A. de Rossi, M. Lauritano, S. Combrié, Q. V. Tran, and C. Husko, Phys. Rev. A **79**, 043818 (2009).
[28] M. F. Yanik, S. Fan, and M. Soljačić, Appl. Phys. Lett. **83**, 2739 (2003).
[29] M. F. Yanik, S. Fan, M. Soljačić, and J. D. Joannopoulos, Opt. Lett. **28**, 2506 (2003).
[30] Y. Dumeige, C. Arnaud, and P. Féron, Opt. Commun. **250**, 376 (2005).
[31] A. Rodriguez, M. Soljačić, J. D. Joannopoulos, and S. G. Johnson, Opt. Express **15**, 7303 (2007).
[32] D. Ramirez, A. W. Rodriguez, H. Hashemi, J. D. Joannopoulos, M. Soljačić, and S. G. Johnson, Phys. Rev. A **83**, 033834 (2011).
[33] F. S. Felber and J. H. Marburger, Appl. Phys. Lett. **28**, 731 (1976).
[34] S. Malaguti, G. Bellanca, A. de Rossi, S. Combrié, and S. Trillo, Phys. Rev. A **83**, 051802 (2011).
[35] K. Ramkumar and K. Nagaraj, IEEE Trans. Circuit Syst. **32**, 732 (1985).
[36] S. Liu, C. Li, J. Wu, and Y. Liu, Opt. Lett. **14**, 713 (1989).
[37] S. Wagner, B. Holmes, U. Younis, A. Helmy, D. Hutchings, and J. Aitchison, IEEE Photonics Technol. Lett. **21**, 85 (2009).
[38] B. Gayral, J. M. Gérard, A. Lemaître, C. Dupuis, L. Manin, and J. L. Pelouard, Appl. Phys. Lett. **75**, 1908 (1999).
[39] C. Husko, A. D. Rossi, S. Combrie, Q. V. Tran, F. Raineri, and C. W. Wong, Appl. Phys. Lett. **94**, 021111 (2009).
[40] C. Koos, P. Vorreau, T. Vallaitis, P. Dumon, W. Bogaerts, R. Baets, B. Esembeson, I. Biaggio, T. Michinobu, F. Diederich, W. Freude, and J. Leuthold, Nat. Photonics **3**, 216 (2009).
[41] B. Lawrence, M. Cha, J. Kang, W. Toruellas, G. Stegeman, G. Baker, J. Meth, and S. Etemad, Electron. Lett. **30**, 447 (1994).